Laser Detection of Pollution

C. K. N. Patel

Summary. Spectroscopic analysis is a useful technique for identifying and quantitatively determining the presence of specific gaseous constituents. Development of high-power tunable lasers has made the spectroscopic technique for detection of trace constituents in the atmosphere very attractive for practical applications. In this article three of the currently used modes for laser detection of pollution are reviewed: (i) long-path measurements, (ii) laser Raman (differential absorption) measurements, and (iii) optoacoustic detection. Progress in the field has been extremely rapid in the last few years and very useful and reliable data on air pollution can now be obtained routinely with the techniques described.

Optical spectroscopy—determination of absorption or Raman spectra of gaseous species (*1*)—has been an accepted method of determining the presence of a molecular species of known properties. Conventionally, on a laboratory scale, spectroscopy is carried out with a blackbody source of radiation such as a globar or a high-pressure arc lamp and a spectrometer (or a set of filters) to monochromatize the radiation for spectral absorption analysis of a sample. The development of tunable high-power lasers has attracted new interest in this old technique. The specific characteristics of the laser which have made the resolution possible are the high degree of monochromaticity and directionality of the laser output and the high powers available. In addition to the detection itself, the specific problem addressed in a given technique is its specificity and immunity from interference from other components in a gaseous mixture. In the spectroscopic studies the specificity is easily acquired by using a radiation source possessing very high resolution and sufficient tunability to obtain a "fingerprint" of the absorption from the desired molecular species for identification. No bigger problem has plagued the conventional blackbody source-spectrometer combination than the need for higher and higher resolution. In the infrared region of the spectrum where the fundamental vibrational-rotational absorption frequencies of most if not all molecules are located, increasing the spectrometer resolution inevitably results in a reduced available radiation flux; hence, sooner or later, one runs into the unsurmountable problem of detector NEP (noise equivalent power, which is a measure of the minimum optical power that can be detected with a given detector). Because the laser radiation line width is determined by quantum (*2*) considerations, the above problem does not arise when a tunable laser source is used. Even under the situation of Doppler line width–limited operation of the absorption measurement systems, where resolution of the order of $1:10^6$ to $1:10^7$ is necessary, the laser source provides enough power output not to be detector NEP limited. The high directionality of the laser brings yet another advantage. In situations requiring either long-path pollution measurements or remote sensing systems, the highly directional nature of the laser allows one to use small-size optical components for transmission as well as reception of the tunable radiation.

Interaction of laser radiation with a molecular species occurs either through absorption or scattering. It is easy to see how the absorption technique can allow us to identify a given molecule. With inelastic or Raman scattering we can obtain a similar fingerprint scattering spectrum for any molecule and obtain a definitive identification. However, for Raman scattering, the cross sections are approximately eight to ten orders of magnitude smaller than those for absorption. Thus in general the absorption measurements are preferred for detection of minor atmospheric constituents. The Raman scattering technique, however, does possess a singular advantage in that the source of radiation does not have to be tunable. The spectral information is obtained by analyzing the scattered radiation with a spectrometer.

Absorption measurements for pollution detection generally fall in three categories: (i) long-path measurements, (ii) remote (single-ended) sensing, and (iii) in situ measurements. To a large extent these three techniques (and their many variations) provide complementary information and are not necessarily competitive. Each one is suited to a particular application and the studies described herein will show the advantages of each of the schemes.

In Fig. 1 I summarize the existing tunable lasers from ~ 4000 angstroms to 40 micrometers and show their average power output. These lasers include dye lasers (*3*), optical parametric oscillators (OPO) (*4*), color center lasers (*5*), tunable diode lasers (*6*), and spin flip Raman (SFR) lasers (*7*). In addition to this wide variety of continuously tunable sources of laser radiation in the visible and the infrared region, we also have a number of molecular gas laser systems which operate on a large number of discretely tunable frequencies in the 4- to 15-μm region. For example, the CO_2 laser (*8*) operates on lines spaced by ~ 2 cm^{-1} in the 9- to 11-μm region; the N_2O laser (*9*) operates on lines spaced by ~ 1 cm^{-1} in the 9.5- to 11.2-μm region; the CS_2 laser (*10*) operates in the 11- to 11.5-μm region on lines separated by ~ 0.2 cm^{-1}; the CO laser (*11*) operates on lines separated by ~ 4 cm^{-1} in the 4.7- to 7.5-μm region; HF and DF lasers (*12*) operate in the 2.8- to 3.4-μm region; HCl and DCl lasers (*13*) operate in the 3.8- to 4.2-μm region; and HBr and DBr lasers (*13*) operate in the 4.3- to 4.6-μm region. Line selection is carried out by means of intercavity grating (or other wavelength selection devices). Isotopic substitution (*14*) in the above molecules further increases the number of discrete lines. Most molecules of interest in pollution detection schemes have their electronic absorption in the ultraviolet—at wavelengths shorter than ~ 4000 Å. While secondary tunable sources do exist here (*15*) (that is, tunable radiation generated by sum frequency mixing or doubling of a tunable dye laser and a fixed frequency laser such as the argon ion laser in the visible) these are not developed far enough to be of significant use in pollution detection. Thus

---

The author is director of the Physical Research Laboratory at Bell Laboratories, Murray Hill, New Jersey 07974.

0036-8075/78/1013-0157$ /0

in general it is the vibrational-rotational spectra of molecules that we have to utilize for the detection and identification of molecular species in pollution. These spectra are to be found between ~ 2 and 15 μm and thus we see that the available tunable laser sources—OPO, color center lasers, diode lasers, and SFR lasers—cover the entire range of interest.

Absorption Measurements

The use of a measured absorption spectrum to identify the constituents of a gas sample relies very heavily on the resolution of the spectrum and the smallest absorption that is measured with a given technique. The former determines the extent to which a constituent can be identified (that is, interference can be rejected from other major or minor constituents in the sample), whereas the latter determines the smallest concentration that can be reliably detected and measured. Since we are studying various techniques for the determination of pollution, both of the criteria are equally important and we will use them for evaluation of each of the specific techniques.

Resolution and interference rejection. At low gas pressures the absorption line widths are limited by Doppler broadening, $\Delta\nu_D$, given by

$$\Delta\nu_D = \frac{\nu_0}{c}\left(\frac{2kTln2}{M}\right)^{1/2} \qquad (1)$$

where ν_0 is the absorption center frequency, c is the velocity of light, k is Boltzmann's constant, T is the gas temperature, and M is molecular mass. For convenience one can simplify the expression to yield

$$\Delta\nu_D = \frac{214.5}{\lambda_0}\left(\frac{T}{M_0}\right)^{1/2} \text{MHz} \qquad (2)$$

where λ_0 is the absorption wavelength in micrometers and M_0 is molecular mass (in atomic mass units). The Doppler widths turn out to be in the range of 30 to 200 MHz for many of the constituents of interest in pollution detection [for example, CH_4, NO, CO, CH_4, NO_2, NH_3, PAN (peroxyacetylnitrate), SO_2], using their fundamental infrared absorption bands in the 2 to 15 μm region. Tunable infrared lasers, such as the diode lasers and the SFR lasers, are capable of providing resolution far in excess of that needed to resolve Doppler line width–limited absorption spectra. Figures 2 and 3 show a spectrum of NO near 5.3 μm obtained with a diode laser (*16*) and a spectrum of 20 parts per million of NO in nitrogen (nominally dry) obtained with an SFR laser (*17*). Sub-Doppler resolution spectroscopy has been carried out with the SFR laser (*18*) but this is not discussed herein. Figures 2 and 3 indicate that the gas pressure is low compared to atmospheric pressure, in order to avoid collision broadening. [The natural broadening contribution from lifetime considerations is a small fraction of the Doppler broadening and is of no consequence in the present discussion. It is important, however, in sub-Doppler spectroscopic studies (*18*).] For an example of collision broadening see Fig. 4, where the H_2O absorption line at 1885.24 cm^{-1} is measured with an SFR laser at two different gas pressures (*19*). The pressure broadening can be a boon or bane depending on the source of radiation that is being utilized for absorption measurements. With continuously tunable laser sources, pressure broadening is clearly detrimental for pressures higher than those at which pressure broadening exceeds the Doppler broadening. With the discretely tunable laser sources, pressure broadening of the absorption line is one of the simplest mechanisms for remedying the problems arising from the general lack of exact coincidences between absorption lines of pollutant molecules and the discrete laser emission lines from the molecular lasers. Again, even with continuously tunable lasers, the option of working at low pressures to obtain high interference rejection is limited by the type of measurement technique that is used. In the case of obtaining measurements in situ where an absorption cell that contains the sample gas can be evacuated, we can easily take advantage of low pressures and increased interference rejection. However, in the case of long-path pollution measurements for terrestrial applications, we can only work at atmospheric pressures.

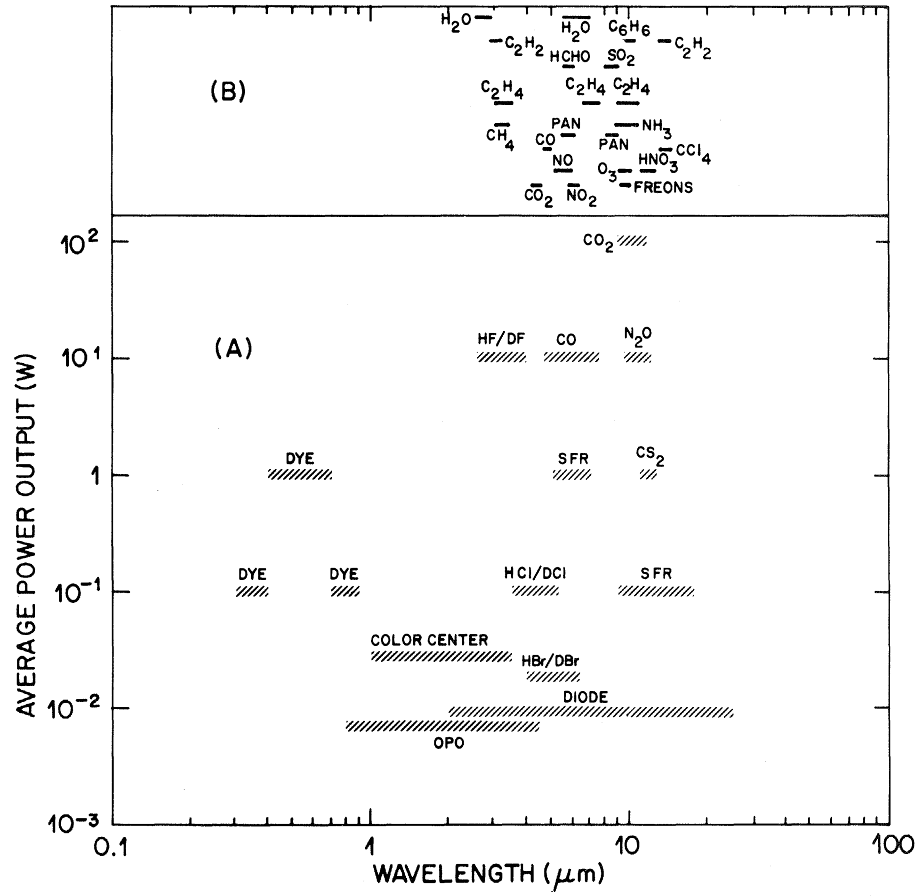

Fig. 1. (A) Summary of approximate average power output plotted against wavelength for a variety of continuously and discretely tunable lasers in the visible and the near infrared region. The output powers denoted on the figure are for typical laboratory-sized lasers. (B) Spectral regions of absorption arising from vibrational-rotational transitions of some typical molecules of interest in pollution detection.

The advantages of continuously tunable laser sources for spectroscopic determination of gaseous pollutants are more obvious than the advantages of discretely tunable laser sources. However, CO_2 and CO lasers, for example, are much simpler to construct, operate, and maintain, than the diode and SFR lasers, and the output power available from the

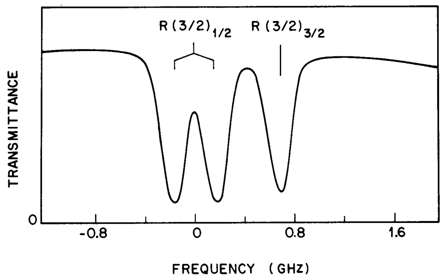

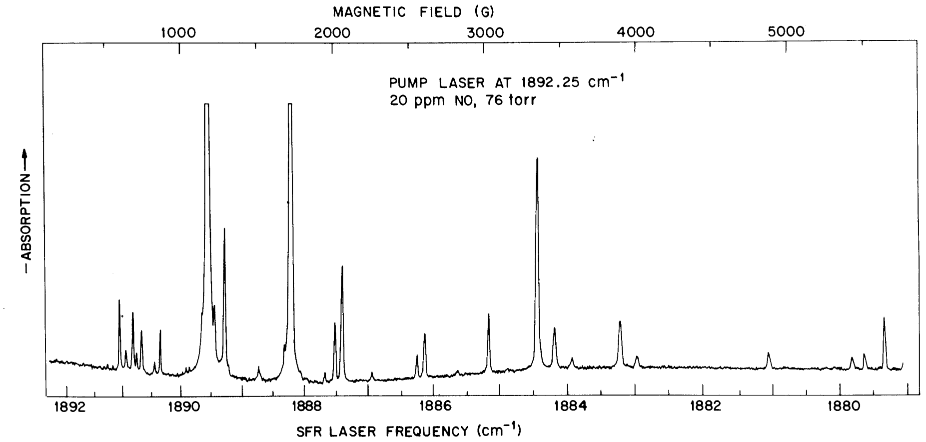

Fig. 2 (left). Absorption spectrum of NO near 1884 cm^{-1}, obtained with a tunable diode laser source, showing the $R(3/2)_{1/2}$ and $R(3/2)_{3/2}$ transitions. The Λ-type doubling of the $R(3/2)_{1/2}$ illustrates the resolution possible with a continuously tunable laser. Note that the absorption lines are Doppler broadened, cell length 5 cm. NO pressure 4 torr, $T = 294$ K. [After Nill *et al.* (*16*)] Fig. 3 (right). Absorption spectrum obtained with an SFR laser for a 20 parts per million NO sample in 76 torr of dry nitrogen. The absorption lines at 1890.5, 1887.5, 1884, and 1883 belong to NO, and the others arise from residual water vapor in the calibration sample (*17*).

discretely tunable laser sources is higher than that from the continuously tunable sources. Thus, in spite of the basic need for operating at high pressures, which makes interference rejection difficult, the discretely tunable lasers have found specific applications in the field of pollution detection. Of course, for long-path measurements where the option of working at low pressures in the primarily Doppler broadened line width region is not available, the discretely tunable molecular lasers are viable sources. For applications, in situ, these lasers can be used for pollution detection applications in specific instances.

Differential absorption measurement. A simple absorption measurement scheme is shown in Fig. 5. The absorption path is a laboratory-sized absorption cell in the case of measurements in situ and is the free air propagation path in the case of long-path measurements. The scheme shown requires the measurement of the reference power (D_1) and transmitted power (D_2) to obtain the absorption coefficient defined by

$$e^{-\alpha l} = \frac{D_2}{D_1} \tag{3}$$

In the case of pollutant species, by necessity its concentration as well as its absorption coefficient, α, will be small and thus Eq. 3 implies a measurement of small change in transmitted power. Experimentally, such a straightforward measurement technique can be used for measuring absorptions $(1 - e^{-\alpha l})$ as small as 10^{-4}. Of course, this assumes that the tunable laser power is large enough so that the NEP of the detectors D_1 and D_2 is not the limiting factor. In other words, the tunable laser power has to be at least 10^4 times the NEP of the detectors. For measurements in situ, the minimum detectability of $\alpha l = 10^{-4}$ is not very useful since even for strong absorbers in the infrared the maximum absorption coefficients are ~ 10^{-2} to 10^{-1} cm^{-1} torr^{-1}. Thus for reasonable path lengths (for detection in situ) of ~ 1 meter the smallest concentration of a trace gas that can be detected is 3×10^{11} to 3×10^{12} cm^{-3}. At atmospheric pressure this detectivity corresponds to a mixing ratio of ~ 10 to 100 parts per billion. For long-path measurements, however, the straightforward absorption measurement technique can provide considerably better sensitivity since path lengths of the order of 0.1 to 1 kilometer can be easily utilized. For a 1-km path length, the detectability can be in the vicinity of 10 to 100 parts per trillion.

Derivative absorption measurement. Instead of measuring the change in the transmitted power level as the frequency, ν, of the tunable laser radiation (Fig. 5) is changed, we can employ a modulation technique. Here the tunable laser radiation frequency has a periodic variation given by

$$\nu(t) = \nu + \delta\nu \sin \omega_m t \tag{4}$$

The modulation frequency ω_m is chosen to be within the frequency response of the detector and the modulation $\delta\nu$ is chosen to be a small fraction of the line width of the molecular transition that is being measured. Instead of measuring the absolute power level with the detector D_2 as was done in the previous section above, we measure the a-c component at frequency ω_m which arises because of the infrequency-dependent absorption in the vicinity of the molecular absorption line. The absorbed power, P_{abs} at a given frequency ν is given by

$$P_{abs} = P_{inc}(1 - e^{-\alpha l}) \tag{5}$$

where P_{inc} is the incident power. For small absorption coefficients, α, Eq. 5 reduces to

$$P_{abs} = P_{inc}(\alpha l) \tag{6}$$

Thus as we tune the laser frequency across the molecular absorption line (assume low pressures and only Doppler broadening) the absorbed power is given by

$$P_{abs}(\nu) = P_{inc} l \alpha_0 \exp\left[-\frac{(\nu - \nu_0)\sqrt{ln2}}{\Delta\nu_D}\right]^2 \tag{7}$$

Thus

$$\begin{aligned}\frac{\delta P_{abs}(\nu)}{\delta t} &= P_{inc}\alpha_0 l \frac{ln2(\nu - \nu_0)}{(\Delta\nu_D)^2} \delta\nu \cos \omega_m t \\ &\quad \exp\left[-\frac{(\nu - \nu_0)\sqrt{ln2}}{\Delta\nu_D}\right]^2 \\ &= P_{abs} \frac{ln2(\nu - \nu_0)}{(\Delta\nu_D)^2} \delta\nu \cos \omega_m t\end{aligned} \tag{8}$$

Thus the absorbed power as well as the transmitted power contain a time varying component both at ω_m and $2\omega_m$. The modulation spectroscopy involves measurement of this component which then gives a measure of absorbed power. The derivative signal thus obtained (*17*) gets around the problem arising from amplitude fluctuations which limits the sensitivity of the technique described in the previous section. The modulation spectroscopy technique, in principle, can be used for measuring absorption as small as 10^{-8} if one assumes that the a-c component of the transmitted power induced by the frequency-dependent absorption of the gas is larger than the NEP of the detector D_2. Output from D_1 can still be used for normalizing the measured a-c component of absorbed power. Since this a-c component is proportional both to the gaseous absorption as well as the incident power, the sensitivity of the modulation technique for measuring small absorption coefficients improves as $1/P_{inc}$ up to the ~ 10^{-8} limit mentioned above. Beyond this level the shot noise generated in the detector D_2 by the large background radiation (that is, the unabsorbed radiation) begins to dominate the operation of the detector and little further improvement is possible by increasing P_{inc}. Hinkley *et al.* (*20*) have given a detailed discussion of the modulation technique and its capability under conditions of pure Doppler broadening (low pressures), pure collision broadening (high pressures), and a mixture of Doppler and collision broadening (intermediate pressures).

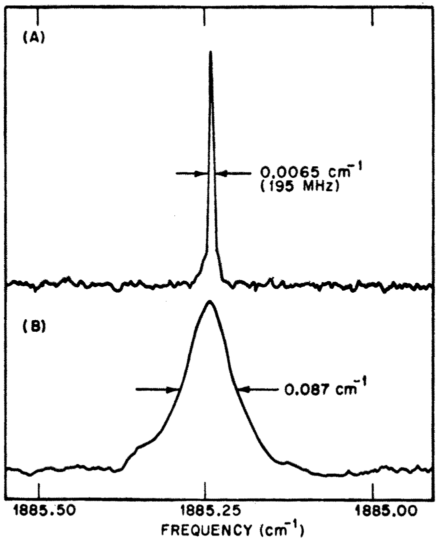

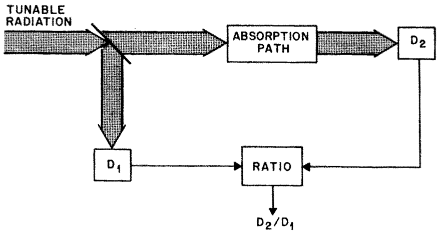

Fig. 4 (left). Absorption spectrum of the $11_{3,9}$ to $10_{2,8}$ (ν_2 band) H_2O vapor line at ~ 1885.24 cm^{-1} obtained with an SFR laser. H_2O in air at (A) $P_{air} \approx 30$ torr, (B) $P_{air} \approx 760$ torr. Pressure broadening effects are clearly seen (*19*). Fig. 5 (right). Simple absorption measurement scheme.

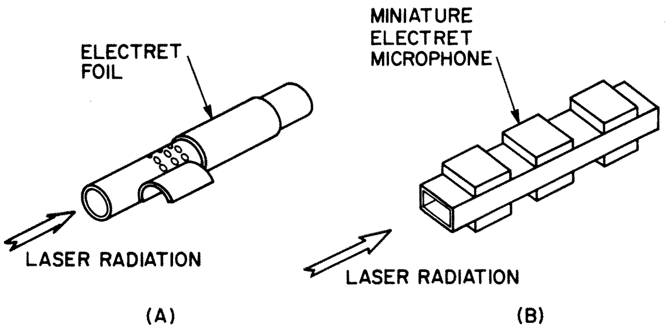

Fig. 6. Construction details of earlier cylindrical OA cell (A), and a recent planar configuration (B) (*27*).

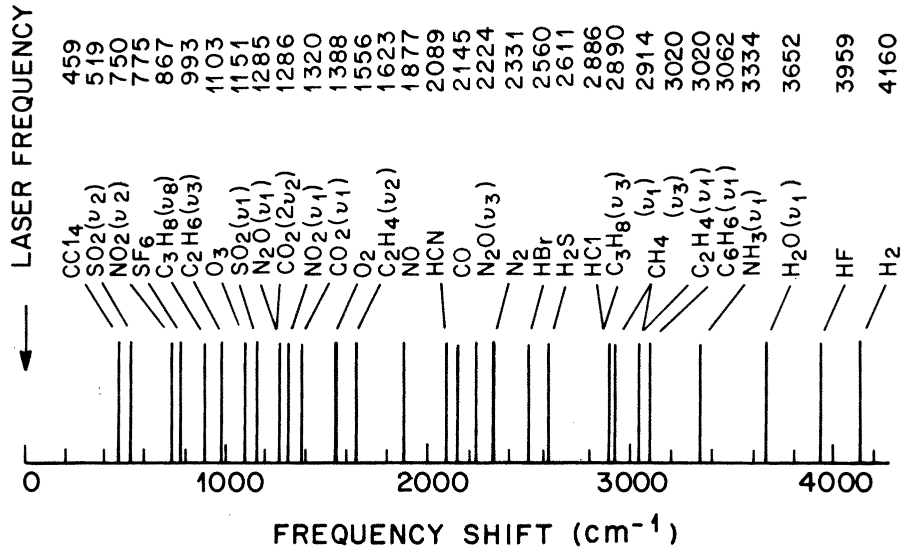

Fig. 7. Frequency shifts of Q-branches of vibrational-rotational Raman spectra of typical molecules of interest in pollution detection. [After Inaba (*30*)]

Optoacoustic detection. The optoacoustic (OA) technique differs in a conceptual manner from the previous two techniques in that in principle no infrared radiation detecting devices are necessary for measuring the absorption. Yet in part the OA technique bears a certain resemblance to the modulation spectroscopy technique discussed above in that both the techniques measure the absorbed power directly. But that is where the similarity ends. The OA technique is primarily a calorimetric technique and is based on the recognition that the fractional amount of incident power lost must remain in the sample itself. The OA method measures directly this amount of power which, in the case of molecular absorption in the infrared region, is left in the form of vibrational excitation of the molecules. The excitation and deexcitation steps can be written as

$$M + h\nu\,(\text{resonant}) \rightarrow M^*\,(\text{excitation}) \qquad (9)$$

$$M^* \xrightarrow{k_{em}} M + h\nu \quad (\text{radiative deexcitation}) \qquad (10)$$

$$M^* + X \xrightarrow{k_{v \rightarrow t}} M + X + KE \quad (\text{nonradiative deexcitation}) \qquad (11)$$

where h is Planck's constant, k_{em} is the rate of radiative emission, $k_{v \rightarrow t}$ is the rate of conversion of vibrational to translational energy, X is a second molecule, atom, or wall involved in the collision with M^*, and KE is kinetic energy. The step shown in Eq. 9 occurs when the frequency of the tunable laser radiation coincides with that of the molecular absorbing transition and represents the loss of photons from the incident beam. Equations 10 and 11 describe two of the primary mechanisms for deexciting the vibrationally excited molecules. In general, in the infrared region, because of the ν^3 factor in the spontaneous emission probability, radiative deexcitation is less important than the nonradiative or collisional deactivation. In Eq. 11, the excited molecule M^* loses its vibrational deexcitation by collision with another body which denotes either another molecular or atomic species or the walls of the absorption cell. During this mode of deactivation the vibrational energy is converted into translational energy of the molecules and corresponds to an increase in the gas temperature.

When the vibrational to translational conversion rate $k_{v \rightarrow t}$ is substantially faster than the spontaneous emission deactivation probability k_{em}, a condition that is readily met for molecular vibrational level relaxation at a pressure of a few torr or higher, we see that most of the energy absorbed in the molecular species goes into an effective heating of the gas. Even at lower gas pressures or for specific molecules where $k_{em} > k_{v \to t}$, we can show that the calorimetric technique we envision here still is useful. This can be seen from a hypothetical unfavorable situation where we find $k_{em} \geq k_{v \to t}$. The first thought that all the energy absorbed by the molecular species will be lost by reradiation is incorrect because the spontaneous emission occurs in 4π steradians, whereas a reasonable absorption cell is in the form of a long narrow cylinder with a small diameter/length ratio. Thus only a small fraction of the reradiated photons are lost through the ends of the cell. Those remaining are intercepted by the cell walls. If the cell walls are not made to be highly reflective, much of the photon flux intercepted by the walls is converted to heat and appears as an increase in the gas temperature. Such a conversion from the internal energy of the molecule to their kinetic energy is not as efficient as, say, the direct collisional deactivation, but is sufficiently efficient that calorimetric detection can be carried at pressures low enough where $k_{em} \gg k_{v \to t}$. At intermediate pressures, the situation is clearly more favorable than the extreme case just described. Thus in a typical situation in the infrared region it is reasonable to find that most, if not all, of the vibrational excitation energy of the molecules is converted to thermal energy in the gas. There is one exception to this generalization, however, and this is the phenomenon of self-induced transparency in which there is forward reemission of the radiation along the well-defined direction of propagation of the incident laser beam.

Calorimetric detection of absorption in solids or liquids is a straightforward matter. One simply measures the rise in the temperature of the medium by using suitable thermometers. In a gaseous medium the change in the gas temperature is best accomplished by measuring the change in pressure that accompanies the rise in the temperature of a gas in a relatively closed absorption cell. Changes in pressure, especially the time-varying ones at some audio frequencies, are easily measured with sensitive acoustic microphones (*21, 22*). This scheme, the OA detection, was first described (*23*) in 1880 to 1881 in connection with conversion of acoustically modulated light into sound for communication purposes. Subsequently, the OA technique has been used, only sporadically, for spectroscopic determination of specific gases.

Since the OA technique directly measures the absorbed power given by Eqs. 5 and 6, the OA signal is proportional to both the absorption coefficient and the incident power. Thus the ability of the OA technique to measure small absorption coefficients improves as $(P_{inc})^{-1}$ with available amount of tunable laser power

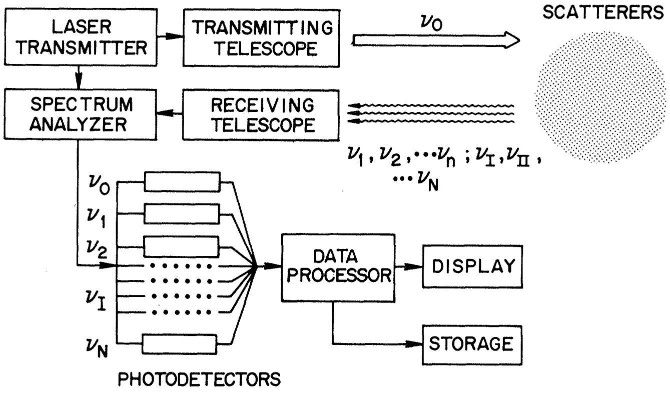

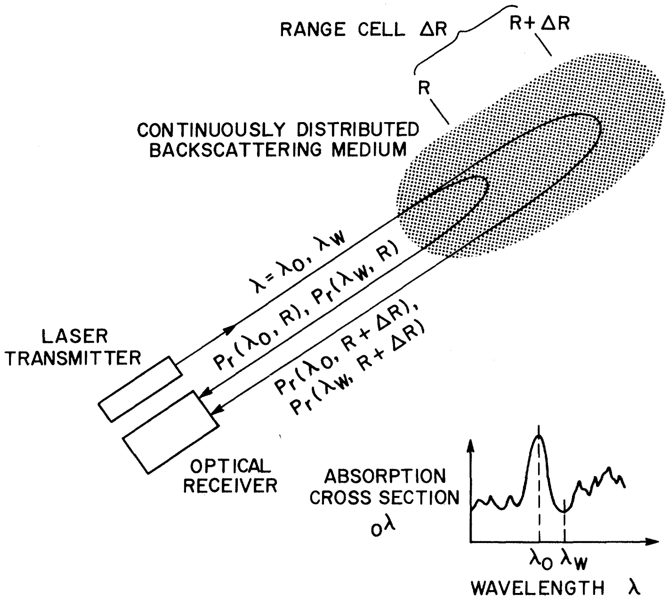

Fig. 8 (left). Schematic diagram of a Raman Lidar system for range-resolved remote pollution monitoring. The spectrum analyzer refers to an optical spectrometer with multiplexed outputs. [After Inaba (*30*)] Fig. 9 (right). Schematic representation of the differential absorption Lidar (DIAL system). [After Collis and Russell (*33*)]

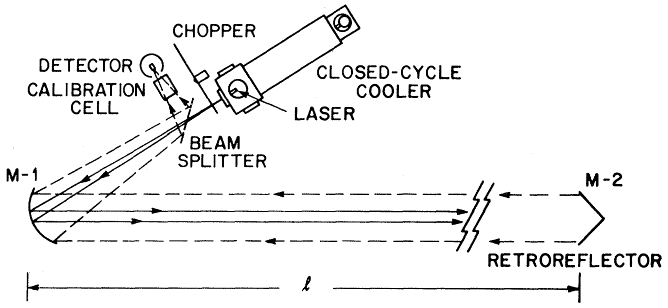

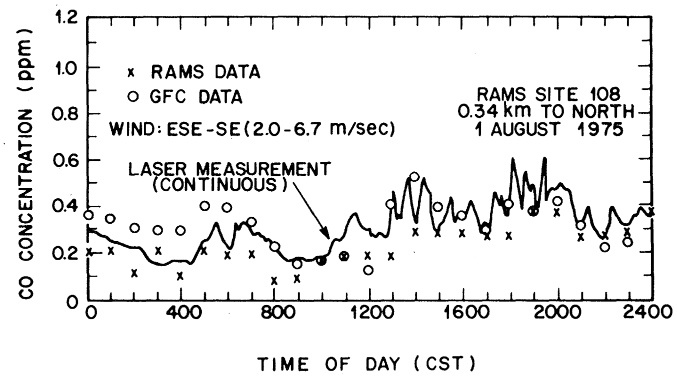

Fig. 10 (left). Schematic of a diode laser (cooled by a closed cycle cooler) based long-path pollution monitoring system with a remote reflector. [After Ku *et al.* (*38*)] Fig. 11 (right). Around--the-clock monitoring of CO over a total path length of 680 meters with a diode laser [After Ku (*38*)] for spectroscopy. There is no fundamental limit to how small an absorption can be measured. With limited amount of incident power, the limitation on the minimum detectable absorption with the OA technique is set by the equivalent NEP and $P_{\min}$ (transducer) of the OA transducer (in the present case an acoustic microphone), and is given by

$$P_{\min}(\text{transducer}) \leq P_{\text{inc}}(1 - e^{-\alpha l}) \qquad (12)$$

The $P_{\min}$ (transducer) is the effective NEP of the entire OA system if one takes into account the conversion of absorbed power into minimum detectable pressure change. This change depends on a variety of factors (*24*) including the microphone response and geometric configuration of the OA cell, for example. Since $P_{\min}$ (transducer) is predetermined once an OA cell is designed, we clearly see that smaller absorption coefficients can be measured by increasing the incident power and that the minimum detectable absorption, $\alpha_{\min}$, varies as $1/P_{\text{inc}}$. In practice, there are other limitations on $\alpha_{\min}$ which arise not from fundamental considerations but from the specific design of the OA cell. For example, the absorption of the incident radiation by the entrance and the exit windows of the absorption cell represents a source of OA signal. However, this signal is in large part independent of the frequency of the incident radiation and hence is not expected to contribute any structure as the laser is tuned across a molecular absorption transition. But this signal, in some sense, is a background signal similar to that in the case of the modulated absorption technique described above. By proper choice of window materials the window absorption can be made as small as 10^{-6} to 10^{-7}. Further rejection against such strong signals can be obtained by (i) using a resonant OA cell (*25*) which discriminates against axial pressure fluctuations by resonating only the radial pressure waves originating in the OA absorption cell, (ii) using appropriate acoustic baffles (*26*) between the windows and the bulk of the absorption cell, and (iii) using windowless OA cells where ambient pressure operation is acceptable. In any case it is important to make sure that none of the incident tunable laser radiation directly impinges on the walls of the OA cell either because of misalignment or improper focusing of the incident radiation. Such an occurrence will result in a large background signal (largely frequency independent). Other considerations that need to be mentioned are that variation of pressure in the OA cell should be kept at a minimum because the transducer response as well as the effect of pressure-induced collision broadening will change the operating characteristics. With proper care in maintaining a constant pressure in the OA cell, we can show that sensitivity of the OA absorption measurement technique (normalized to incident power) remains constant.

The construction of the OA absorption measuring cell is straightforward. Figure 6 shows two arrangements that have been successfully used. In Fig. 6A we show an older version (*21*) of the OA cell in which the microphone is cylindrical in shape and is constructed out of a thin-walled metallic cylinder with a perforated wall and a thin Mylar film, aluminized on the outside, which is wrapped around the metallic cylinder. The metal cylinder and aluminized outer layer of Mylar film form a capacitor microphone. (Frequently, precharged electret foil is used instead of the Mylar film.) This cell construction provided enough sensitivity to detect ~ 2 × 10^8 NO molecules per cubic centimeter when the tunable laser power was provided by an SFR laser. Figure 6B shows an improved version (*27*) which uses special electret microphones with built-in preamplifiers. The new geometry and microphones have led to an improvement of a factor of ~ 10 in the above sensitivity. Now we are able to measure absorption coefficients as small as 10^{-10} cm^{-1} in a cell length of ~ 10 cm. This corresponds to a minimum detectable NO concentration of ~ 1 to 2 × 10^7 cm^{-3}. The sensitivity was also checked by careful measurements (*28*) of controlled direct heat input into the cell by using a heater wire along the axis of the cell and passing an a-c electrical current through the wire.

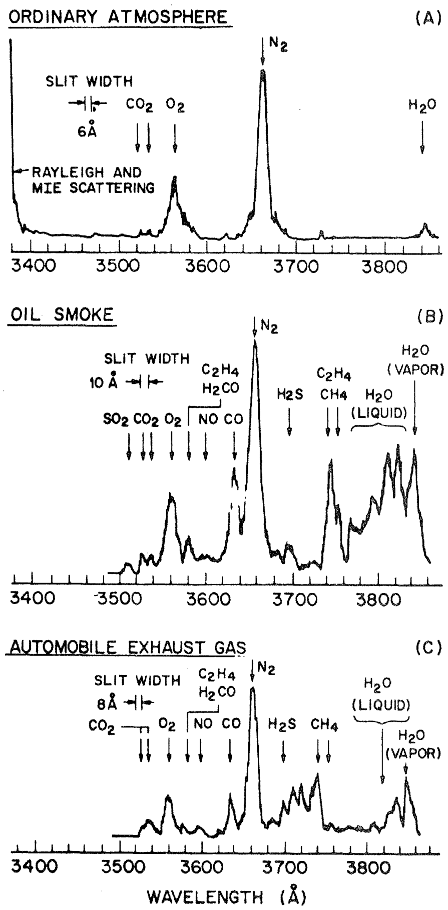

Fig. 12. Raman Lidar measurements of (A) ordinary atmosphere, (B) oil smoke, and (C) automobile exhaust gas. [After Inaba (*43*)]

Another characteristic of the OA absorption measurement technique is the very wide dynamic range that is available. The OA absorption measurement limitation at the low end is set by the equivalent NEP of the OA cell and the available tunable laser power. At present this low-end limit is an αl ~ 10^{-9}. This limit improves with increasing the input power. At the high end two limits are seen. The first one is the saturation of OA signal from the microphones, because the "sound level" generated in the OA cell increases when an increasing amount of incident power is absorbed owing to increasing α. This limitation, however, is not a fundamental one in that for a given absorption coefficient α, the absorbed power in the OA cell can be reduced by reducing the incident power (see Eq. 5) by use of appropriate calibrated optical attenuators. The second limitation, on the other hand, is a fundamental one and it arises from the fact that with increasing absorption coefficient, at some point the intensity of the incident radiation can no longer be considered constant through the OA cell because a substantial fraction of the incident laser radiation is being absorbed. The acoustic power generated cannot possibly exceed the optical input power. In practice, the OA cell response begins to saturate when the absorbed power approaches ~ 10 percent of the incident power. Thus the upper limit for a linear response of the OA cell is set at αl ~ 0.1, implying a dynamic range for the OA absorption measurement technique of about eight orders of magnitude. Experimentally we have verified the linearity of the response of an SFR laser-OA spectrometer over seven to eight orders of magnitude for detection of NO. This dynamic range allows the same instrumentation to be used for ambient (very low levels) trace constituent detection as well as for source (very high levels) emission detection for pollution monitoring applications in situ.

Light Scattering Measurements

Raman scattering. Raman scattering of a monochromatic or nearly monochromatic radiation by solids, liquids, and gas has long been used as a tool for obtaining spectroscopic information about the structure of the medium (*29*) and for obtaining information about qualitative and quantitative presence of specific constituents. I will discuss here only gaseous media but the data are general enough to be applicable to solids as well as to liquids. When an input radiation at frequency ν_0 is incident on relatively particulate-free gaseous sample, two mechanisms give rise to scattering of ν_0. The first is Rayleigh scattering (or inelastic scattering) which occurs at the same frequency as the input radiation and in general carries no information about the structure of the gaseous medium. The second mechanism which gives rise to the scattering of the input radiation is Raman scattering, that is, inelastic scattering from characteristic excitations such as electronic, vibrational, and rotational excitations of the gaseous medium. Thus the scattered radiation, ν_s, contains components at a frequency lower (Stokes) and at a frequency higher (anti-Stokes) than the incident frequency, given by

$$\nu_s = \nu_0 \pm \nu_r \tag{13}$$

where ν_r is the frequency of the characteristic excitation of the gaseous species. Just as a complete absorption measurement of a gaseous sample can be used as a fingerprint for identifying its constituents, a complete Raman scattering spectrum can be used as a fingerprint for similar determination. Figure 7 shows a partial summary of vibrational Raman shifts for a few molecular species of interest in pollution measurements (*30*). In general, the Raman scattering cross sections are eight to ten orders of magnitude smaller than the absorption cross sections and the Raman scattering cross sections vary as ν_0^4. Thus the use of a high incident radiation frequency is desirable for effective use of Raman scattering as means of pollution detection.

Figure 8 shows a schematic diagram of the laser Raman system for pollution detection (*30, 31*). The laser transmitter, typically, consists of a high-power pulsed laser in the visible or the near ultraviolet region, such as doubled or tripled yttrium aluminum garnet laser, pulsed nitrogen laser, or pulsed dye laser. The pulsed laser output, at a frequency ν_0 is collimated with a telescope of reasonable size and is transmitted in the direction of the atmospheric constituents. The Raman scattered light which contains the information about the constituents and their concentration is radiated in 4π steradian, and thus a large telescope near the transmitter will collect a fraction of the Raman scattered radiation. The amount of radiation collected depends on the distance at which the scattering centers are located and the size of the receiving telescope. There is an important distinction between the absorption measurement schemes described in the preceding section and the Raman scattering scheme. Unlike the absorption measurement scheme which yields information about a single frequency at a time, the return Raman scattered light contains information about *all* the constituents in the scattering volume simultaneously. The desired fingerprint in the absorption scheme is obtained by tuning the laser source frequency, whereas the same information in the Raman scattering scheme is obtained by a frequency analysis of the return signal with a spectrometer which preferably has multiplexed output so that more than one return frequency can be monitored at one time. It is important to point out, however, that multiplexing reduces data collection time only if we are reasonably sure of the qualitative composition of the scatterers and wish to obtain quantitative information about them. If an interference from an unknown scatterer is a possibility, then the spectrometer may have to be continuously tuned to obtain shape information about the fingerprint to eliminate or account for the interference.

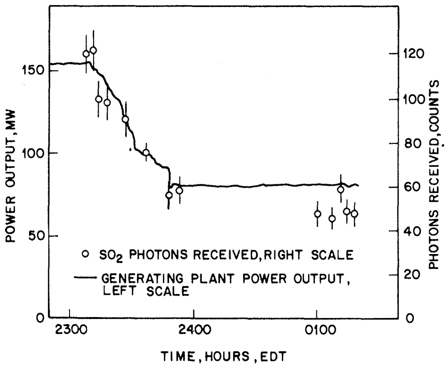

Fig. 13. Correlation between SO_2 emission from a power generating plant effluent, measured using a Raman Lidar system, and the plant's power output. [After Melfi *et al.* (*44*)]

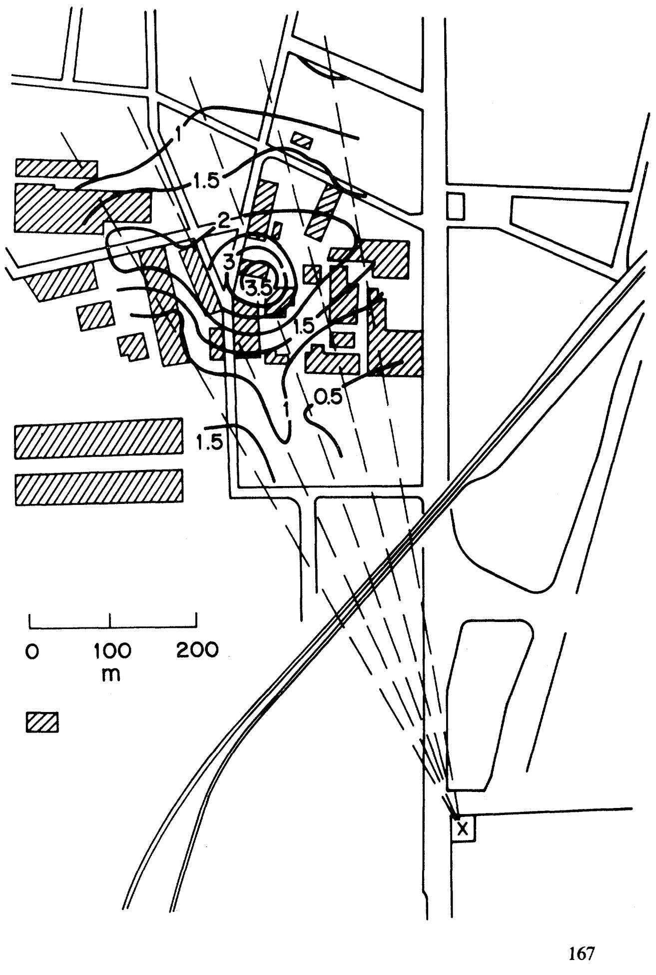

Fig. 14. The distribution of NO_2 in parts per million over a chemical factory obtained through DIAL measurements carried out with a tunable dye laser source at location marked with X. Measurements were carried out at an altitude of ~45 meters along the directions shown. [After Rothe *et al.* (*49*)]

The laser Raman scattering scheme called Lidar is primarily a long-path measurement scheme. But here, in contrast

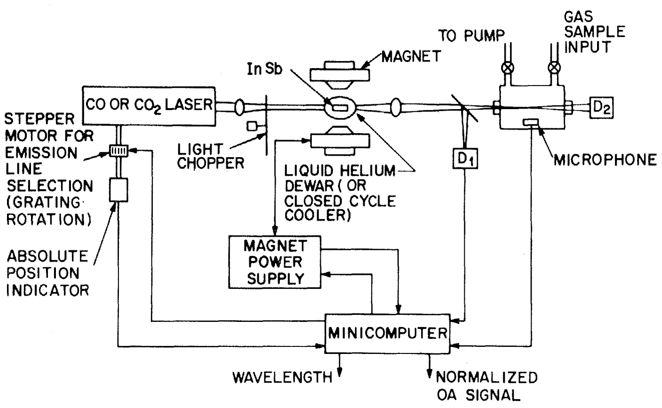

Fig. 15. Diagram of an SFR laser–OA spectrometer configured for in situ pollution detection.

to the long-path absorption measurement schemes described earlier, we have the additional possibility of obtaining range information. Such information is not possible with absorption schemes which give us primarily the average information about the entire path length. The range information with Lidar is obtained by a temporal analysis of the return Raman signal. Since, in general, pulsed lasers are used for the primary transmission, the range information is simply obtained by measuring arrival times of various signals. The range resolution possible with Lidar is limited by the width of the transmitted laser pulse. For a pulse length of, say, 100 nanoseconds, range resolution of ~ 30 meters is possible.

The Lidar scheme is a single-ended scheme compared to the absorption measurement schemes in the previous sections. These absorption schemes cannot be considered single-ended even though one may argue that detection of the transmitted radiation will be carried out near the transmitter by having a remote mirror. The absorption measurement schemes become truly single-ended when reflection from topographical objects or Mie scattering from particulates is used as a remote "mirror." The former can be used in continuous long-term monitoring of pollution from a satellite-based tunable laser system which looks down toward the earth and uses natural objects for reflected radiation. The latter scheme, which has much promise, is a combination of the scattering and absorption scheme. Mie scattering of particulates is well understood in terms of its frequency dependence, and thus differential absorption of the intervening atmosphere (by using a tunable laser source) is possible in a time-resolved single-ended absorption measurement scheme which has, in part, advantages of both the Lidar and absorption measurement schemes.

For all its multiplexing and range advantages, the Lidar suffers seriously from the smallness of the Raman scattering cross section. For example, typical absorption cross sections for molecular pollutants of interest are ~ 10^{-18} cm^2 per molecule (*20*), whereas the Raman scattering cross sections are typically 10^{-28} to 10^{-31} cm^2 per molecule (*30*). Thus the Lidar scheme finds practical applications for probing pollutant levels in the source environments, for example, single-ended examination of stack effluents. Typical sensitivities are ~ 10 to 100 parts per million at a distance of ~ 100 meters for SO_2 and NO_2 detection (*30*). Some enhancement of the Raman scattering cross section is possible when the transmitted frequency lies close to an electronic transition of a particular species to be detected. This then requires the use of a tunable laser source, removing some of the advantages of simpler instrumentation associated with Lidar. By means of tunable dye lasers, it is also possible to monitor given molecular or atomic species by observing the return signal corresponding to resonance fluorescence. Such resonance fluorescence schemes, in principle, hold promise for airborne or balloon-borne Lidar for probing stratospheric and topospheric constituents. Ground-based resonance fluorescence measurements include detection of Na and K atoms in the stratosphere.

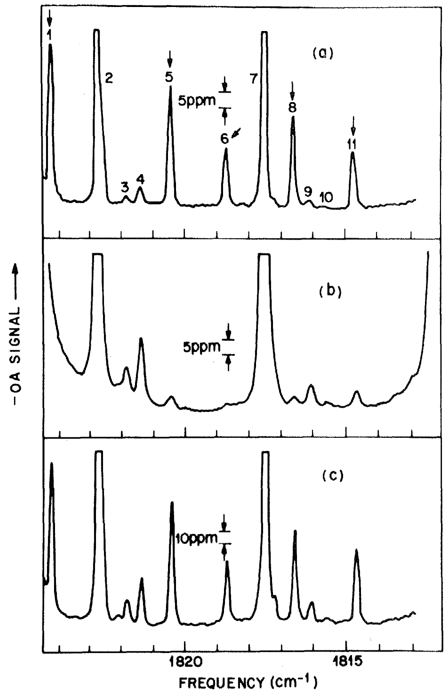

Fig. 16. (a) Optoacoustic signal plotted against magnetic field (B) for NO calibration sample (20 parts per million). (b) Optoacoustic signal plotted against B for ambient air in an active parking lot. (c) Optoacoustic signal plotted against B for automobile exhaust gases.

Scattering and differential absorption. The differential absorption Lidar (DIAL) technique is a combination of the Lidar and long-path absorption measurements (*32*). Using a pulsed tunable laser source such as a parametric oscillator one can obtain detectable scattered signal back from a continuously distributed Mie scattering medium (*33*) (see Fig. 9). By making measurements of the return signal at the transmission ν_0, which includes the information about the scattering medium as well as the absorption in the intervening path, we can obtain long-path absorption data. Here we assume that the general nature of the backscatterer is known and thus the backscattering dependence on transmitted frequency can be predetermined. We also assume that the tuning of the laser source is sufficiently rapid so that no change in the backscattering centers take place. It is evident that this scheme is ideally suited to monitoring pollution over industrialized urban centers where particulates form an important part of pollution. Again, the temporal data of the return signal contains range information (*33*). Since the estimated sensitivities for various pollutants are intermediate between those for long-path transmission measurements and the Raman Lidar, the differential absorption Lidar promises to be useful for single-ended measurements over polluted urban areas.

Measurements of Molecular Pollutants

Having discussed some of the typical techniques for measurements of molecular pollutants I now turn to application of these techniques to specific problems in pollution monitoring. The samples I have chosen include monitoring of specific ambient constituents averaged over long paths by means of either a double-ended or a single-ended system which uses a remote retroreflector; short-path length, source-level pollutant monitoring; single-ended remote Raman scattering measure-

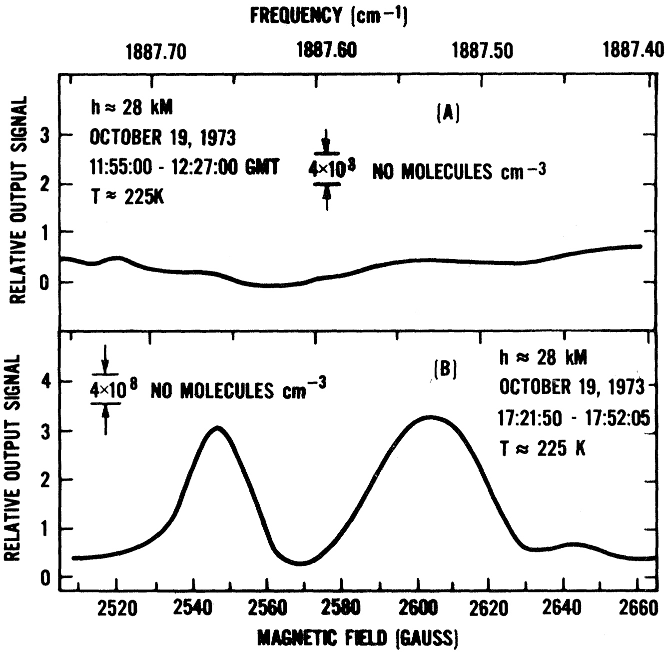

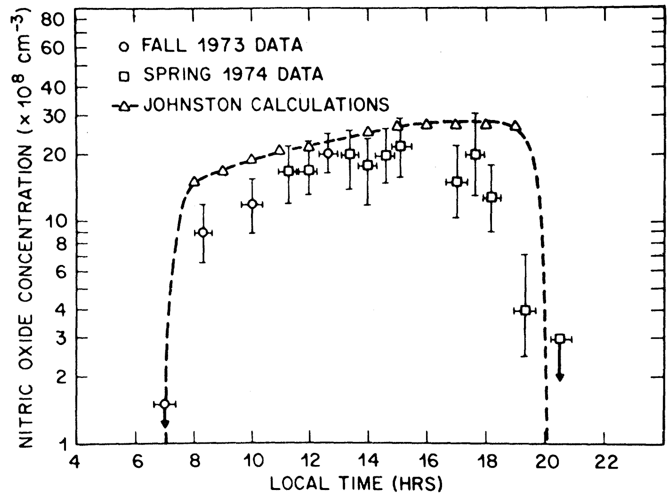

Fig. 17 (left). (A) Optoacoustic signal plotted against B at 28 km, before sunrise. (B) Optoacoustic signal plotted against B at 28 km, at noon. Fig. 18 (right). The concentration of NO plotted against time at ~28 km.

ments of source emission; remote single-ended pollution monitoring of ambient and source levels by means of elastic backscattering and differential absorption; measurements of both source and ambient pollution concentration in situ; and in situ measurements of pollutants in the stratosphere. I have attempted to give an overall picture of the applications of lasers in pollution detection. Further details can be found in reviews of the specific techniques.

Long-path monitoring of pollution. Monitoring of pollution over long-path lengths is a useful means of obtaining the average concentration of a given constituent between the two points. When the distances are commensurate with the typical "cell-size" in modeling of dispersion of pollutants for various sources, long-path measurements can yield data crucial for establishing the reliability and the validity of the models. I am arbitrarily making the distinction between long-path monitoring and measurements in situ that is not based on the length of the sample but on the basis of the requirement or lack thereof of containing the sample in a closed absorption cell. Long-path measurements can be carried out with either a double-ended system consisting of a tunable (either continuously or step tunable) laser source at one end and a detector at the far end of the long path, or a pseudo single-ended system where the source laser and the detector are at the same end of the long path and the light is reflected back at the distant end by using a retroreflector. In essence, this method pollution monitoring is utilized in free atmosphere at ambient pressures where the pressure broadening of the absorption lines is likely to lead to overlap of absorption lines (and resultant interference) from different constituents of the air comprising the transmission medium. The techniques used here are either the straightforward differential absorption scheme or the derivative absorption measurement scheme. A further measurement scheme that could have important long-term implications is the heterodyne detection scheme in which a tunable local oscillator is used for measuring signals reflected from distant topographic objects; by this method one measures either absorption or emission of infrared radiation from hot gases (for example, stack gas). Both of these schemes have been proposed for measurements of stratospheric components with the sun being used as the background blackbody source either with a ground-based system or a balloon or a satellite-based system (*34*). Using a tunable diode laser as a local oscillator and sun as the blackbody source, Frerking and Muehlner (*35*) have measured O_3 concentration in the stratosphere. That the sensitivity of such a technique is excellent can be ascertained from the detection of CO_2 in the martian and venusian atmospheres (*36*) and NH_3 in Jovian atmosphere (*37*) by means of a ground-based heterodyne radiometer in which a CO_2 laser was used as a local oscillator.

Hinkley and his colleagues (*20*) have carried out a series of impressive studies to evaluate a bistatic (pseudo single-ended in the nomenclature of this article) long-path pollution monitoring system shown schematically in Fig. 10. The measurements (*38*) have involved determination of CO and NH_3 in field measurements in Granite City, Illinois, and NO measurements in Kendall Square, Cambridge, Massachusetts. The tunable laser in these experiments consisted of a PbS_xSe_{1-x} semiconductor diode laser which was cooled down to the necessary operational cryogenic temperatures with a closed cycle cooler. The optical system included an off-axis parabolic mirror and a retroreflector as shown. A liquid N_2-cooled InSb detector was used, and a short-path cell provided the necessary calibration. To minimize problems arising from interference, a number of CO absorption lines (for CO detection studies) were scanned and carefully evaluated. Problems that might be caused by thermal fluctuations in the atmosphere were partially circumvented by derivative spectroscopy. Figure 11 shows a typical round-the-clock monitoring of CO concentration over a 0.68-km path length. For comparison, point-sampling measurements obtained with a gas chromatograph and a gas filter correlation system are shown. The good agreement between the laser long-path data and the point sampling results was consistent with the existing meteorological conditions. Further experiments on the monitoring of NO during rush hour in Cambridge show clearly the correlation with increased internal combustion engine vehicular traffic which is an important source of NO emission.

Although the pressure broadening at atmospheric pressure gives rise to problems associated with interference when we use continuously tunable lasers it also allows us to use discretely tunable lasers such as CO_2 and CO for monitoring

Table 1. Laser lines and sensitivities.

Detection	Calibration sample			
	NH_3 (1000 ppm)	NO_2 (100 ppm)	H_2O (10000 ppm)	HCN (1000 ppm)
CO laser line	$P_{16-15}(7)$	$P_{20-19}(14)$	$P_{24-23}(15)$	$P_{27-26}(12)$
ν(cm^{-1})	1729.76	1605.32	1504.24	1442.15
λ(μm)	5.7812	6.2293	6.6479	6.9341
OA signal	124	150	4.6	115

specific constituents. To a lesser extent, He/Ne laser line at 3.39 μm and visible ion lasers can also be used for monitoring certain pollutants. Measurements have been made of NO_2 over a 3.4-km path by means of an argon ion laser (*39*), O_3 measurements with a CO_2 laser (*40*), and NO measurements with a CO laser (*34*). A discretely tunable laser is also susceptible to interference problems especially if the qualitative composition of the air path is unknown. However, the ease of operation of molecular lasers such as CO_2 and CO make them attractive for certain applications.

Source level pollution monitoring by means of differential absorption. Source level monitoring of gaseous pollutants by differential absorption techniques is a logical adjunct to the ambient level measurements. The major difference lies primarily in the total path length. The real time analysis is especially suited for applications such as monitoring of automobile (or other vehicle) exhausts (*41*) under a variety of operating conditions and stack gas monitoring. Both discretely tunable as well as continuously tunable lasers can be used, although most of the current systems utilize continuously tunable diode lasers. Because of the high concentrations of the pollutants emitted, typically in the 100 to 1000 parts per million range, path lengths of the order of a meter are sufficient for obtaining reliable measurements with time resolution of fractions of a second.

Stack effluents have also been measured by the long-path scheme by Hinkley (*41*) using a Pb_xSn_{1-x} Te diode laser and by Kuhl and Spitschan (*42*) using a tunable ultraviolet dye laser. The detection is made easier here by the high concentration of pollutants, but it is also made difficult by the high density of particulate emission from the stack. A somewhat different scheme was used by Kuhl and Spitschan (*42*) who determined SO_2 concentration in the plume emanating from a smokestack by measuring ultraviolet absorption arising from electronic transitions of SO_2. These authors estimate a detection limit of $<$ 1 part per million of SO_2 for a path length of 1 km.

Raman Lidar measurements. Because the Raman scattering cross sections in general are smaller than the absorption cross sections by eight to ten orders of magnitude, the Raman Lidar scheme is in general applicable only to source level rather than ambient level detection of pollutant molecules. With the initial observation (*31*) of Raman scattering signal from atmospheric N_2 and O_2 in 1967, the technique has now been extended to molecular pollutant gases of interest such as SO_2, CO_2, H_2S, and kerosene vapor. Inaba and Kobayasi (*43*) used a Q-switched ruby laser as a source of high-power radiation in their Raman Lidar measurements of SO_2 and CO_2 in the effluent of smokestack, oil smoke plume, and automobile exhaust—at a distance of 30 meters. Figure 12 shows the observed Raman spectrum from the analysis of the return scattered light from ordinary atmosphere, oil smoke plume, and automobile exhaust, where a pulsed N_2 laser at ~ 3370 Å is used as the source. The peaks due to C_2H_4, NO, CO, and H_2O are unequivocally identified; however, interference problems prevent such definite identification of H_2CO, H_2S, and CH_4. The ease of making single-ended measurements without the use of tunable lasers for determination of pollutants is the very strength of the Raman Lidar technique. The measurement apparatus has been subsequently installed in a van making the Raman Lidar scheme a practical mobile system for remote stack effluent determinations.

Melfi *et al.* (*44*) have used a pulsed ruby laser system for the measurement of SO_2 in the smokestack plume of an electricity generating plant. Their measurements of SO_2 emission in the effluent show a good correlation with the power output of the generating plant. The results in Fig. 13 represent a data collection time of ~ 100 seconds for each of the points except the one at 23:35 to 23:45 where the averaging time was 500 seconds corresponding to 500 laser pulses.

The discussion of Raman Lidar measurements of atmospheric pollutants cannot be complete without the mention of resonance fluorescence measurements of stratospheric atomic sodium and potassium. Bowman and co-workers (*45*) detected a column density of Na of 6×10^{13} m^{-2} at a height of 80 to 100 km. These measurements have been extended by a number of groups for observing seasonal variation of Na concentration and evidence of its stratification. Measurements have also been extended to atomic potassium (*46*) whose column density measured $\sim 9 \times 10^{11}$ m^{-2}.

Elastic backscattering and differential absorption. Use of topographic objects

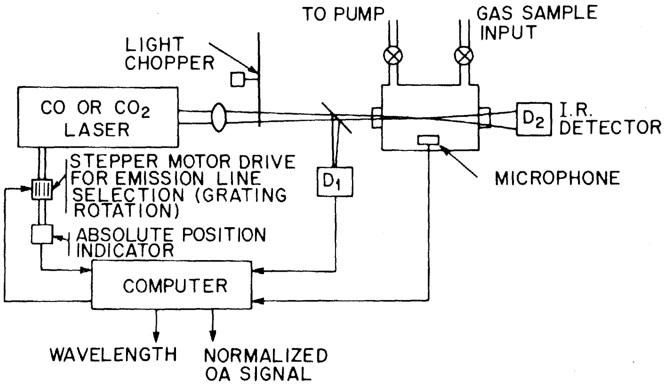

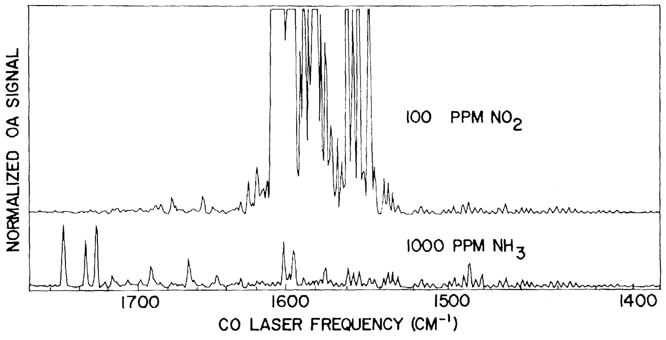

Fig. 19 (left). Step-tuned CO_2/CO laser-OA pollution detection spectrometer. Fig. 20 (right). (Top) Optoacoustic signal plotted against a step-tuned CO laser wavelength for 100 parts per million of NO_2 in N_2. (Bottom) Optoacoustic signal plotted against step-tuned CO laser wavelength for 1000 parts per million of NH_3 in N_2.

or Mie scattering (or diffuse reflections from any other target) as a retroreflector makes this scheme considerably more versatile than the quasi single-ended scheme involving a "cooperative" reflector. In other aspects this scheme differs very little from the long-path absorption technique described above. Unlike the Raman Lidar scheme where a single nontunable laser source is capable of providing both qualitative and quantitative information on the constituents of the target medium, the present scheme requires at least one wavelength per constituent. Under the most ideal circumstances, fixed-frequency lasers chosen to match the absorption frequencies of appropriate pollutants can be used as sources of radiation for this technique (Fig. 9). Murray *et al.* (*47*) have used discrete lines of a DF laser to detect HCl, CH_4, and N_2O in a remote sample chamber. Using a DF laser energy of ~100 to 150 millijoules per pulse for $P_2(3)$ line to detect HCl, $P_1(9)$ line to detect CH_4, and $P_3(7)$ line to detect N_2O, they are able to estimate sensitivity, in parts per million per kilometer, of 0.05, 6.0, and 0.24 for HCl, CH_4, and N_2O, respectively, for a topographic target (in this case a juniper shrub) located at ~300 meters from the laser transmitter. For N_2O, Murray *et al.* (*47*) have been able to detect a man-made plume replacing the remote sample chamber. The DIAL scheme possesses range resolution capabilities when use is made of backscattering from aerosols and particulates instead of the reflection from topographic objects. Murray *et al.* (*47*) further anticipate that with this system both total-burden (distance integrated) as well as range-resolved pollution measurements should be possible for ranges up to 10 km.

To avoid problems of interference that plague any discretely tuned laser system for absorption measurements, one can estimate the amount of interference and then compensate for it. However, this requires that the exact concentration of the interfering species also be known—a problem that cannot be resolved if the sample contains an unknown or new constituent. A continuously tunable laser, of course, avoids the problem or at least minimizes it. Byer and his colleagues (*48*) have constructed a tunable parametric oscillator as the source laser for DIAL. They have detected CO and SO_2 in a remotely located absorption cell using diffusely reflected radiation for foliage. The CO and SO_2 measurements were carried out for a target distance of 107 and 195 meters, respectively. For SO_2, they report a detection capability of <1 part per million per kilometer and expect a sensitivity of ~ 50 parts per billion per kilometer with improved parametric oscillators. In spite of the obvious promise of the infrared DIAL no actual field measurements of pollutants have yet been reported.

Table 2. Interference-limited sensitivity.

Component	Sensitivity limit	Interference (component)
HCN	0.5 ppm	5 percent H_2O
NH_3	0.5 ppm	10,000 ppm NO_2
NO_2	0.2 ppb	

An outstanding example of visible region DIAL measurements is the determination of NO_2 over the city of Cologne. Rothe and his colleagues (*49*) used a dye laser tunable between 4550 and 4700 Å—a region within which the NO_2 electronic absorption spectrum exhibits a structure that can be used as a fingerprint. Using a pulse energy ~1 millijoule in a 300-nanosecond pulse, and Mie scattering for getting the return reflection, Rothe *et al.* have measured NO_2 concentrations as low as 0.2 part per million up to a distance of 4 km. Figure 14 shows a range-resolved two-dimensional plot of NO_2 concentration. The contours indicate the source of the NO_2, in this case a chemical factory. The laser pulse width, τ, of 300 nanoseconds gives a minimum range resolution of $c\tau/2 \sim 50$ meters. Rothe *et al.* have also made direct DIAL measurements of a smokestack plume which showed a lateral extent of 200 to 300 meters at a distance of 300 meters from the exit of the stack.

When use is made of a pulsed tunable infrared laser, a region where most of the common pollutants have their fundamental vibrational-rotational absorption frequencies, the DIAL technique holds promise of being a practical technique for single-ended remote pollution monitoring.

Pollution Detection with OA Spectroscopy

Under ideal circumstances, the tunable SFR laser is best suited for pollution measurements because the continuous tunability allows one to obtain a complete fingerprint absorption of the species of interest and to identify as well as quantitatively measure its concentration in the presence of other gaseous constituents at much higher concentrations. The step tunable CO or CO_2 lasers, on the other hand, offer the simplicity of their being primary laser sources, and they are simple to operate, and they have very high power outputs.

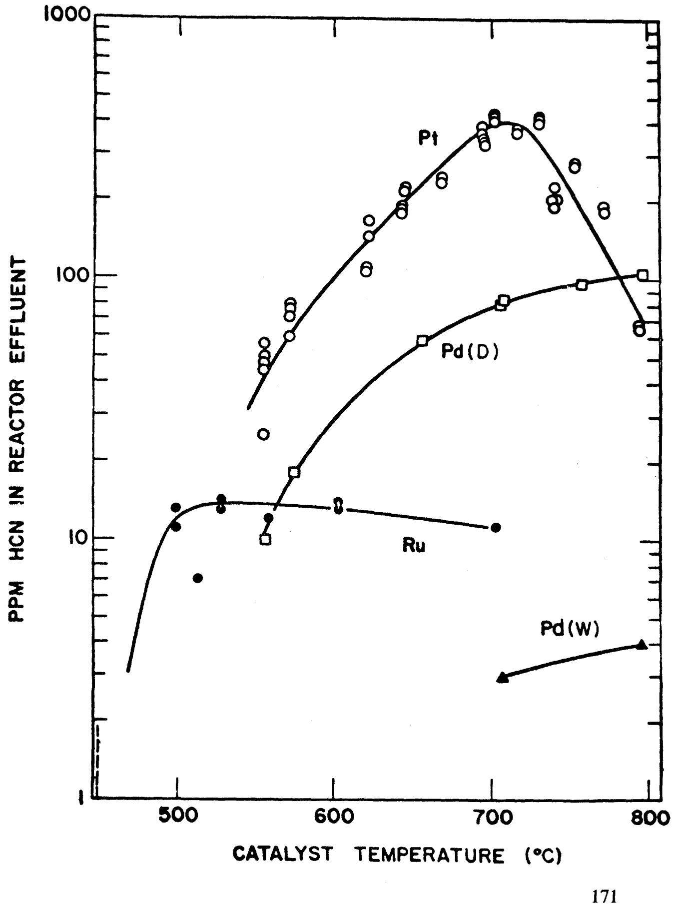

Fig. 21. The HCN yield as a function of catalyst temperature for Ru, Pd, and Pt II catalysts. The Pd(W) shows HCN yield for standard inlet gas mixture (5 percent CO, 0.5 percent H_2, 0.3 percent NO, balance He) with 3.5 percent added H_2O.

Spin flip Raman laser–OA absorption pollution detection. Figure 15 shows an experimental setup for measuring gaseous pollutant concentration by means of an SFR laser–OA absorption measurement system. The primary data output from the system is the OA absorption signal as a function of the magnetic field used for tuning the SFR laser. The magnetic field values are eventually converted to SFR laser frequency, ω_{SFR}, if one uses the tuning relation

$$\omega_{\mathrm{SFR}} = \omega_{\mathrm{pump}} - g\mu_{\mathrm{B}}B \qquad (14)$$

where ω_{pump} is the pump laser frequency, g is the g value of the electrons in the SFR laser crystal, μ_{B} is Bohr magneton, and B is the magnetic field. Unfortunately, g is a slowly decreasing function of B and thus tuning of the frequency is less than linear in B. However, detailed measurements exist which allow accurate conversion of known B to the SFR laser frequency (*7*).

Ambient and source level pollution detection. One of the first uses of a tunable laser-based OA technique for pollution detection (*50*) was reported in 1971. This consisted of ambient (under a variety of situations) as well as source level (automobile exhaust, in the present situation) measurements of nitric oxide. In Fig. 16a the lines marked with arrows arise from absorption due to NO, whereas the remaining ones are H_2O absorption lines arising from the residual H_2O in the nominally dry calibration sample. Figure 16b shows ambient air analyzed in a fairly active parking lot. From the strength of the NO absorption line No. 8, which shows the least interference from H_2O, the NO concentration in the parking lot is estimated to be ~2 parts per million. Figure 16c shows an analysis of automobile exhaust gases. (Note that the sensitivity scale has been changed.) The particular automobile exhaust is seen to contain ~80 to 100 parts per million of NO. Because of the enormous signal/noise ratio for NO detection available in the SFR laser–OA detection technique, the measurements shown in Fig. 16, b and c, are carried out in real time with a typical time for each measurement of less than 1/10 second.

Detection of minor constituents in the stratosphere. The ultralow level detection capability described above has found an important application to the real time measurement of minor constituents in the stratosphere, whose chemistry as well as composition, especially regarding the trace gases, has recently been the subject of theoretical studies and model-making. The catalytic destruction of stratospheric ozone by NO has become a controversial issue since the expansion of commercial SST flights in the stratosphere. The concentrations of NO and NO_2 are thought to play a crucial role in the ozone balance (*51*). Expected NO and NO_2 concentrations are $\sim 10^9$ mole/cm^3 and the known ozone concentration (at ~28 km) is $\sim 10^{12}$ mole/cm^3. The following reactions summarize the primary NO/NO_2–O_3 interactions (only primary ones):

$$NO_2 \xrightarrow{h\nu} NO + O \qquad (15)$$

$$NO_2 + O \rightarrow NO + O_2 \qquad (16)$$

$$O_3 + NO \rightarrow NO_2 + O_2 \qquad (17)$$

These reactions emphasize the importance of solar radiation in NO/NO_2 catalytic destruction cycle of ozone. To provide any reliable observational basis for the importance of NO and NO_2 in ozone balance, we must know not only the concentrations of these compounds but also their diurnal variation which provides proper check on the time constants for the reactions described in Eqs. 15 to 17.

To obtain the necessary data on NO, the entire SFR laser–OA absorption system (similar to that in Fig. 15) was enclosed in a capsule and flown to an altitude of 28 km for real time measurements in situ (*52*). Figure 17, A and B, shows the OA spectrum of ambient air (at 28 km) analyzed before sunrise and at local noon. There is a lack of NO before sunrise and a large concentration of NO at noon. Figure 18 summarizes all the data compiled on two such balloon flights. The measurements provide (i) the absolute concentration of NO and (ii) its diurnal variation. Many details of the model proposed above are confirmed (*52*).

Recent discussions of stratospheric chemistry have dealt with the effect of freons (*53*) on ozone balance through a Cl/ClO catalytic destruction of ozone. The fundamental absorption band of ClO is measured (*54*) to be at ~11 μm. Use of the OA absorption measurement technique with isotopically substituted CO_2 laser should allow us to carry out fundamental measurements on ClO and its diurnal variation in the stratosphere.

Step-tunable laser–OA absorption pollution detection. It is easy to see how a spectroscopic technique that uses a continuously tunable source (laser) can provide accurate determination of a given molecular species. Both CO_2 and CO lasers provide a multitude of step-tunable (by incorporating a grating with the laser cavity) laser lines in the 10- and 5-μm regions, respectively. At low gas pressures, where the molecular absorption lines are essentially Doppler broadened, an exact coincidence between any of the step-tunable laser lines and an absorption line of a given molecular species will only be accidental and thus, in general, the step-tunable laser–OA absorption technique may be of no practical significance. However, pressure broadening of absorption lines of molecules can be advantageously used for obtaining absorption of laser lines which are close to a given absorption time but which are not exactly coincident. The difficulty is that in general we may not be able to obtain an entire fingerprint pattern of absorption of the molecule and that absorption from another molecule may also give rise to an interference signal when pressure broadening is a necessary requirement for the success of the technique. (The overriding reason for the use of step-tunable fixed lasers, as opposed to the SFR lasers described in the previous section, is that the experimental apparatus can be simplified.) The interference problem is largely solved by making measurements, successively, with several different step-tuned laser lines, and creating a matrix of absorption signals obtained from the OA cell. Then, with the use of an on-line computer (see Fig. 19) one can derive the concentration of each one of the gaseous constituents, making use of a calibration matrix obtained by using known calibration gas samples. Figure 20, top and bottom, points out the importance of the proper choice of CO laser lines for detection of NO_2 and NH_3 with minimum interference from each other. It has been shown earlier (*55*) that with this technique one can detect many of the common industrial pollutants at parts per billion levels of their concentrations.

We have studied (*56*) the effluent from a catalyst, nominally designed for oxidation of CO to CO_2. The catalyst was tested under reducing conditions with inlet gases reflecting typical concentrations of CO, NO, and H_2O from untreated automobile exhaust. Analysis showed that sizable conversion of NO to HCN and to NH_3 takes place under the reducing conditions and pointed to some possible problems associated with the catalytic treatment of automotive exhaust. The HCN measurements carried out with the step-tunable CO laser–OA spectrometer showed that we are able to determine HCN at concentrations lower than parts per million in the presence of very large concentrations of interfering gases such as NO_2 and H_2O. Tables 1 and 2 give the laser lines used and the sensitivities for the detection of HCN. These data are obtained by rapid scan of the CO laser frequencies under computer control (*57*)

(Data General Eclipse) which allows continuous optimization of operating conditions and data collection as well as data manipulation for direct quantitative determination of various pollutant gases. As opposed to gas chromatography techniques, we are able to provide transient measurements which are important in the analysis of the reactions as well as in the study of time-dependent poisoning of the catalysts (*58*). Figure 21 shows HCN concentrations in the effluent as a function of the catalyst temperature for three different catalysts. Transient studies of HCN and NH_3 emission have also been carried out to determine effects of the addition of oxygen to the inlet gases. Recent studies (*59*) of actual automobile catalysts under operating conditions substantiate our original findings where the step-tunable CO laser–OA spectrometer played a crucial role.

Other examples of the discretely or continuously tunable laser OA detection scheme include the measurement of ambient concentrations of CO with a CO laser operating on the 1 to 0 vibrational-rotational band (*60*) and the measurement of SO_2 at the parts per billion concentration (*61*) with an optical multipass OA absorption cell and a dye laser as the source.

Conclusions

With the tremendous advances in the capabilities of continuously and discretely tunable lasers in the visible and the infrared region of the spectrum in the last decade, we have seen an intense activity in the use of the lasers for pollution detection applications. From the examples of techniques and applications that I have summarized it is evident that virtually every aspect of pollution monitoring with lasers is under active study, and many of the methods are being used in practical pollution monitoring tasks. The new technology of lasers has made it possible to measure and monitor trace gaseous constituents that could not be measured previously. Although the level of automation in laser based systems does not yet equal that of the more conventional systems, the new systems are nonetheless being used for routine as well as novel applications.

References and Notes

1\. See, for example, G. Herzberg, *Molecular Spectra and Molecular Structures* (Van Nostrand, New York, 1945 to 1966), vols. 1–3.

2\. C. H. Townes, in *Advances in Quantum Electronics*, J. R. Singer, Ed. (Columbia Univ. Press, New York, 1961), p. 3; see also W. R. Bennett, Jr., *Appl. Opt. Suppl.* **1**, 24 (1961).

3\. C. V. Shank, *Rev. Mod. Phys.* **47**, 649 (1975).

J. A. Giordmaine and R. C. Miller, *Phys. Rev. Lett.* **14**, 973 (1965); for recent advances, see R. L. Byer, in *Tunable Lasers and Applications*, A. Mooradian, T. Jaeger, P. Stokseth, Eds. (Springer-Verlag, New York, 1976), pp. 70–80.

5\. L. F. Mollenauer and D. H. Olson, *Appl. Phys. Lett.* **24**, 386 (1974).

6\. See, for example, the review by I. Melngailis and A. Mooradian, in *Laser Applications in Optics and Spectroscopy*, S. Jacobs, M. Sargent, J. F. Scott, M. Scully, Eds. (Addison-Wesley, New York, 1975), pp. 1– 51.

7\. C. K. N. Patel and E. D. Shaw, *Phys. Rev. Lett.* **24**, 451 (1970); C. K. N. Patel, in *Proceedings of the Royal Society Meetings on Light Scattering in Physics and Chemistry* (22–24 February 1978, in press); in *Fundamental and Applied Physics*, M. Feld, A. Javan, N. Kurnit, Eds. (Wiley, New York, 1973), pp. 689–722; in *Laser Spectroscopy*, R. C. Brewer and A. Mooradian, Eds. (Plenum, New York, 1974), pp. 471–491; see also C. R. Pidgeon and S. D. Smith, *Infrared Phys.* **17**, 515 (1977).

8\. C. K. N. Patel, *Phys. Rev. Lett.* **12**, 588 (1964); *ibid.* **13**, 617 (1964); ______, P. K. Tien, J. H. McFee, *Appl. Phys. Lett.* **7**, 290 (1965); see also reviews by A. J. DeMaria, *Proc. IEEE* **61**, 731 (1973); O. R. Wood, *ibid.* **62**, 355 (1974).

9\. C. K. N. Patel, *Appl. Phys. Lett.* **6**, 12 (1965).

10\. ______, *ibid.* **7**, 273 (1965).

11\. ______ and R. J. Kerl, *ibid.* **5**, 81 (1964).

12\. T. F. Deutsch, *ibid.* **10**, 234 (1967).

13\. ______, *IEEE J. Quantum Electron.* **QE-3**, 419 (1967).

14\. See, for example, the compilation of laser wavelengths, in *Tables of Laser Lines in Gases and Vapors*, R. Beck, W. Englisch, K. Gurs, Eds. (Springer-Verlag, New York, 1978).

15\. See, for example, F. B. Dunning, *Laser Focus* **72** (May 1978), and references cited therein.

16\. K. W. Nill, F. A. Blum, A. R. Calawa, T. C. Harman, *Chem. Phys. Lett.* **14**, 234 (1972).

17\. C. K. N. Patel, in *Coherence and Quantum Optics*, L. Mandel and E. Wolf, Eds. (Plenum, New York, 1973), pp. 567–593.

18\. ______, *Appl. Phys. Lett.* **25**, 112 (1974).

19\. ______, *Phys. Rev. Lett.* **28**, 649 (1972).

20\. E. D. Hinkley, R. T. Ku, P. L. Kelley, in *Laser Monitoring of the Atmosphere*, E. D. Hinkley, Ed. (Springer-Verlag, New York, 1976), pp. 238–295.

21\. L. B. Kreuzer, *J. Appl. Phys.* **42**, 2934 (1971).

22\. E. L. Kerr and J. A. Atwood, *Appl. Opt.* **7**, 915 (1968); M. E. Delaney, *Sci Prog. (London)* **47**, 459 (1959); L. G. Rosengren, *Appl. Opt.* **14**, 1960 (1975).

23\. A. G. Bell, *Proc. Am. Assoc. Adv. Sci.* **29**, 115 (1880); J. Tyndall, *Proc. R. Soc.* **31**, 307 (1881); W. C. Rontgen, *Philos. Mag.* **11**, 308 (1881).

24\. See the review of fundamental considerations that determine the NEP of microphones for OA detection by L. B. Kreuzer, in *Optoacoustic Spectroscopy and Detection*, Y-H Pao, Ed. (Academic Press, New York, 1977), pp. 1– 25.

25\. The use of acoustic resonances for increasing sound amplitude from an OA cell was first described by A. G. Bell, *Philos. Mag.* **11**, 510 (1881). Recent experiments with resonant OA cells are described by C. F. Dewey, Jr., R. D. Kamm, C. E. Hackett, *Appl. Phys. Lett.* **23**, 633 (1973).

26\. C. F. Dewey, Jr., *Opt. Eng.* **13**, 483 (1974).

27\. C. K. N. Patel and R. J. Kerl, *Appl. Phys. Lett.* **30**, 578 (1977).

28\. C. K. N. Patel, in preparation.

29\. C. V. Raman, *Ind. J. Phys.* **2**, 387 (1928).

30\. H. Inaba, in *Laser Monitoring of the Atmosphere*, E. D. Hinkley, Ed. (Springer-Verlag, New York, 1976), pp. 153–236, and references cited therein.

31\. D. A. Leonard, *Nature (London)* **216**, 142 (1967).

32\. R. M. Schotland, E. E. Chermack, D. T. Cheng, in *Proceedings of the First International Symposium on Humidity of Moisture* (Reinhold, New York, 1964), p. 569; R. M. Schotland, *J. Appl. Meteorol.* **13**, 71 (1974).

33\. R. L. Byer and M. Garbuny, *Appl. Opt.* **12**, 1496 (1973). See also the review articles by R. L. Byer, *Opt. Quantum Electron.* **7**, 147 (1975) and R. T. H. Collins and P. B. Russell, in *Laser Monitoring of the Atmosphere*, E. D. Hinkley, Ed. (Springer-Verlag, New York, 1976), pp. 71–151.

34\. R. T. Menzies, in *Laser Monitoring of the Atmosphere*, E. D. Hinkley, Ed. (Springer-Verlag, New York, 1976), pp. 297–353.

35\. M. A. Frerking and D. J. Muehlner, *Appl. Opt.* **16**, 526 (1977).

36\. D. W. Peterson, M. A. Johnson, A. L. Betz, *Nature (London)* **250**, 123 (1974); A. L. Betz, M. A. Johnson, R. A. McLaren, E. C. Sutton, *Astrophys. J.* **208**, L141 (1976); M. A. Johnson, A. L. Betz, R. A. McLaren, E. C. Sutton, C. H. Townes, *ibid.*, p. L145.

37\. T. Kostiuk, M. J. Mumma, J. J. Hillmen, D. Buhl, L. W. Brown, J. L. Feris, D. L. Spears, *Infrared Phys.* **17**, 431 (1977).

38\. R. T. Ku, "Diode Laser System to Measure Trace Gases by Long Path Infrared Absorption," *MIT Lincoln Laboratory Report, November 1977*. See also R. T. Ku, E. D. Hinkley, J. O. Sample, *Appl. Opt.* **14**, 854 (1975).

39\. D. C. O'Shea and L. G. Dodge, *Appl. Opt.* **13**, 1481 (1974).

40\. W. A. McClenny, R. E. Baumgardner, Jr., F. W. Baity, Jr., R. A. Gray, *J. Air Pollut. Control Assoc.* **24**, 1044 (1974).

41\. E. D. Hinkley, *Opto-electronics* **4**, 69 (1972).

42\. J. Kuhl and H. Spitschan, *Opt. Commun.* **13**, 6 (1975).

43\. H. Inaba and T. Kobayasi, *Opto-electronics* **4**, 101 (1972); see also S. Nakahara, K. Ito, S. Ito, A. Fuke, S. Komatsu, H. Inaba, T. Kobayasi, *ibid.*, p. 169.

44\. S. H. Melfi, M. L. Brumfield, R. W. Storey, Jr., *Appl. Phys. Lett.* **22**, 402 (1973).

45\. M. R. Bowman, A. J. Gibson, M. C. W. Sandford, *Nature (London)* **221**, 456 (1969); M. C. W. Sandford and A. J. Gibson, *J. Atmos. Terr. Phys.* **32**, 1423 (1970); A. J. Gibson and M. C. W. Sandford, *ibid.* **33**, 1675 (1970).

46\. F. Felix, W. Kleenside, G. Kent, M. C. W. Sandford, *Nature (London)* **246**, 345 (1973).

47\. E. R. Murray, J. E. van der Laan, J. G. Hawley, *Appl. Opt.* **15**, 3140 (1976).

48\. T. Hennigsen, M. Garbuny, R. L. Byer, *Appl. Phys. Lett.* **24**, 242 (1974); R. A. Baumgartner and R. L. Byer, *Opt. Lett.* **2**, 163 (1978).

49\. K. W. Rothe, U. Brinkmann, H. Walther, *Appl. Phys.* **3**, 115 (1974); *ibid.* **4**, 181 (1974).

50\. L. B. Kreuzer and C. K. N. Patel, *Science* **173**, 45 (1971).

H. Johnston, *ibid.*, p. 517; P. J. Crutzen, *J. Geophys. Res.* **76**, 7311 (1971).

52\. C. K. N. Patel, E. G. Burkhardt, C. A. Lambert, *Science* **184**, 1173 (19 E. G. Burkhardt, C. A. Lambert, C. K. N. Patel, *ibid.* **188**, 1111 (1975); C. K. N. Patel, *Opt. Quantum Electron.* **8**, 145 (1976).

53\. M. J. Molina and F. J. Rowland, *Nature (London)* **249**, 810 (1974).

54\. R. T. Menzies, J. S. Margolis, E. D. Hinkley, R. A. Toth, *Appl. Opt.* **16**, 523 (1977).

55\. L. B. Kreuzer, N. D. Kenyon, C. K. N. Patel, *Science* **177**, 347 (1972).

R. H. J. Voorhoeve, C. K. N. Patel, L. E. Trimble, R. J. Kerl, *ibid.* **190**, 149 (1975).

57\. I thank R. H. Rabiner of Data General Corp. for invaluable help and advice about the computer during the course of these experiments.

R. J. H. Voorhoeve, C. K. N. Patel, L. E. Trimble, R. J. Kerl, *Science* **200**, 761 (1978).

59\. R. L. Bradow and F. D. Stump, *SAE (Soc. Automot. Eng.) Tech. Paper 770367* (1977); U.S. Environmental Protection Agency, Office of Air and Waste Management, *Review of HCN Emission Data for 1977 Model Year Certification Vehicles* (Washington, D.C., 8 September 1976).

60\. R. Gerlach and N. M. Amer, *Appl. Phys. Lett.* **32**, 228 (1978).

61\. K. P. Koch and W. Lahmann, *ibid.*, p. 289.